

*2 May*  
X-644-73-378

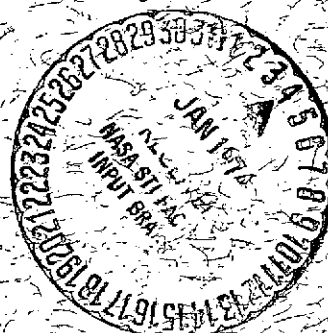
PREPRINT

NASA TM X-70537

SURFACE FEATURES ON MARS:  
GROUND-BASED ALBEDO  
AND RADAR COMPARED  
WITH MARINER 9  
TOPOGRAPHY

HERBERT FREY

DECEMBER 1973



(NASA-TM-X-70537) SURFACE FEATURES ON  
MARS: GROUND-BASED ALBEDO AND RADAR  
COMPARED WITH MARINER 9 TOPOGRAPHY (NASA)  
CSCL 03B  
35 p HC \$3.75

N74-13567

Unclass  
G3/30 = 24505

GFC

— GODDARD SPACE FLIGHT CENTER —

GREENBELT, MARYLAND

SURFACE FEATURES ON MARS: GROUND-BASED  
ALBEDO AND RADAR COMPARED WITH  
MARINER 9 TOPOGRAPHY

Herbert Frey

Planetology Branch  
Laboratory for Space Physics  
Goddard Space Flight Center  
Greenbelt, Maryland 20771

and

Astronomy Program  
University of Maryland  
College Park, Maryland 20740

ABSTRACT.

Earth-based albedo maps of Mars were compared with Mariner 9 television data and ground-based radar profiles to investigate the nature of the bright and dark albedo features. Little correlation was found except at the boundaries of classical albedo features, where some topographic control is indicated. Wind-blown dust models for seasonal and secular albedo variations are supported, but it is not clear whether the fines are derived from bright or dark parent rock. Mars, like the Earth and Moon, has probably generated two distinct types of crustal material.

INTRODUCTION.

Earth-based observations of Mars reveal a surface of dark and bright regions and two seasonally-variable pole caps. While the polar caps are known to consist mostly of frozen carbon dioxide (Neugebauer, et al., 1971; Kliore, et al., 1972), the nature of the bright and dark regions is much less certain. Mariner 9 television pictures and supporting experiments have revealed some information about the physical relationship between bright and dark areas, and many observations of seasonal and secular changes in these areas can be understood in terms of a dynamic, aeolian transport of material over the surface. The fundamental differences between dark and bright albedo features remains unsolved, despite more than a century of reliable earth-based observations.

Dark areas undergo seasonal and non-seasonal alterations in shape, size and albedo. Two hypotheses survive to explain these changes: the Biological Hypothesis and the Wind-Blown Dust Model. Decreasing albedo of dark areas in the springtime hemisphere is explained by the former theory as the response of vegetation to the changing temperature and humidity conditions; longer-term changes would indicate mass extinction or the filling of a newly-available, habitable region. Regeneration of dark areas following extensive dust storms is explained as the growth of plants through the new layer of dust, or simply as the "shaking off" of dust from leaves and stems. Öpik (1966) has discussed this model in some detail.

Transport of bright, fine particles onto or off underlying dark regions can also explain the observed albedo effects; seasonal winds and longer-term climatic changes account for the deposition and removal of the dust (Sagan and Pollack, 1969; Sagan, et al., 1971; Sagan, et al., 1972;

Sagan, et al., 1973). The advantage to this model is that it is subject to test; biological models are ad hoc, as differences in the unknown life forms from their terrestrial counterparts can be invoked to explain minor discrepancies between theory and observation. This is not so of the Wind-Blown Dust Model: once enough is known about the Martian atmospheric structure, wind regimes and surface morphology, definitive predictions must be reconciled with observations. It is a testimony to this model that it has so well survived the data returned from the Mariner 9 mission.

The Wind-Blown Dust Model does not directly imply any information about the compositional nature of the classical albedo features. The IRIS experiment on board Mariner 9 indicated a high ( $\sim 60\%$ )  $\text{SiO}_2$  content for the suspended (bright) particles during the global dust storm (Hanel, et al., 1972). Sagan and his coworkers (Sagan and Pollack, 1969; Sagan, et al., 1971) consider the albedo differences to be principally a difference in particle size: bright areas have a mean particle size some 10's of microns while dark areas consist of a mixture of particles (large, less mobile particles and exchangeable, smaller particles) with a mean size several 100 microns. Ferric oxides, and in particular limonite compounds, have been suggested as a major constituent of the surface by some authors (e.g., Sagan, et al., 1965). Evidence cited includes a sharp rise in spectral reflectivity from 0.4 to  $0.7\mu$ , the presence in some spectra of a weak absorption feature near  $0.85\mu$  (the "limonite band"), and polarization comparisons with terrestrial samples by Dollfus (1961). Others (Salisbury, 1966; Van Tassel and Salisbury, 1964) argue that limonite is unreasonable as a major constituent on geological grounds and (Lowman

and Tiedemann, 1971) is contrary to experience in bright terrestrial deserts. Sinton (1967) and Younkin (1966) find little spectral evidence for limonite. Rea and O'Leary (1965) suggest the polarization data admit a wider variety of rock types than allowed by Dollfus (1961). Binder and Cruikshank (1966) and Binder and Jones (1972) suggest limonite stain on lithic soils as the explanation for the color of Martian deserts. Spectral reflectivity differences are found between bright and dark areas by McCord and Westphal (1971): absorption features near  $1.0\mu$  vary in strength and position as a function of albedo. Oxidized basalts are suggested as constituents of the Martian surface on the basis of laboratory comparisons with these spectral reflectivity curves (Adams and McCord, 1969). Masursky (1973) finds morphological evidence for basaltic flows on the flanks of the large Martian shield volcanoes, and suggests compositional variations among the flows on the basis of their structural characteristics. The extensive sparsely-cratered plains in the bright northern hemisphere of Mars (McCauley, et al., 1972) bear a strong similarity to the known basaltic mare flows on the moon (Masursky, 1973 ; Carr, 1973).

Both the Moon and the sparsely-vegetated deserts of the Earth display a two-fold albedo distribution. In the lunar case, it is the strong compositional differences between highlands and maria that cause the albedo differences (see, e.g., Adler, et al., 1973). In the Sahara desert high areas are chiefly dark, exposed bedrock, while lower areas are brighter, consisting of depositional quartz and silicate sands (Lowman and Tiedemann, 1971).

The above review indicates that little is known of the compositional nature of the classical albedo features on Mars. Albedo differences may

be due to chemical or mineralogical differences, to particle size differences, or to a combination of these. This paper examines the regional geologic relations between albedo features and surface topography in an attempt to decide whether composition or particle size is the major factor responsible for the classical Martian features.

ALBEDO AND REGIONAL STRUCTURE.

Direct comparison between ground-based albedo maps of Mars and Mariner 9 television imagery is now possible. The 1:25,000,000 shaded relief map prepared by the U.S.G.S. at Flagstaff (Figure 1) was overlain by a transparency of the Mariner Mars '71 Planning Chart prepared at the University of Texas under the direction of de Vaucouleurs (Figure 2). Regional comparisons between albedo and terrain are discussed below.

The southern hemisphere of Mars is dominated by old, heavily-cratered plains (Carr, et al., 1973; McCanley, et al., 1972). This is also the hemisphere in which lie most of the prominent dark albedo features. The northern hemisphere consists chiefly of bright, smooth, mare-type plains units (Carr, 1973; Carr, et al., 1973), relatively sparsely cratered. Mariner 9 radio-occultation data (Kliore, et al., 1973; Kliore, et al., 1972) indicates that the southern hemisphere averages some 3-4 kilometers higher than the northern hemisphere of the planet, except at the poles. In this sense, a correlation does exist: dark areas are found mainly in the high, heavily-cratered half of the planet; the north is dominated by lower-lying bright smooth plains. A similar coarse correlation was noted by Inge and Baum (1973) for parts of Mars, especially those lying in the Mare Sirenum-Cimmerium region. The classical feature Hellas fits this

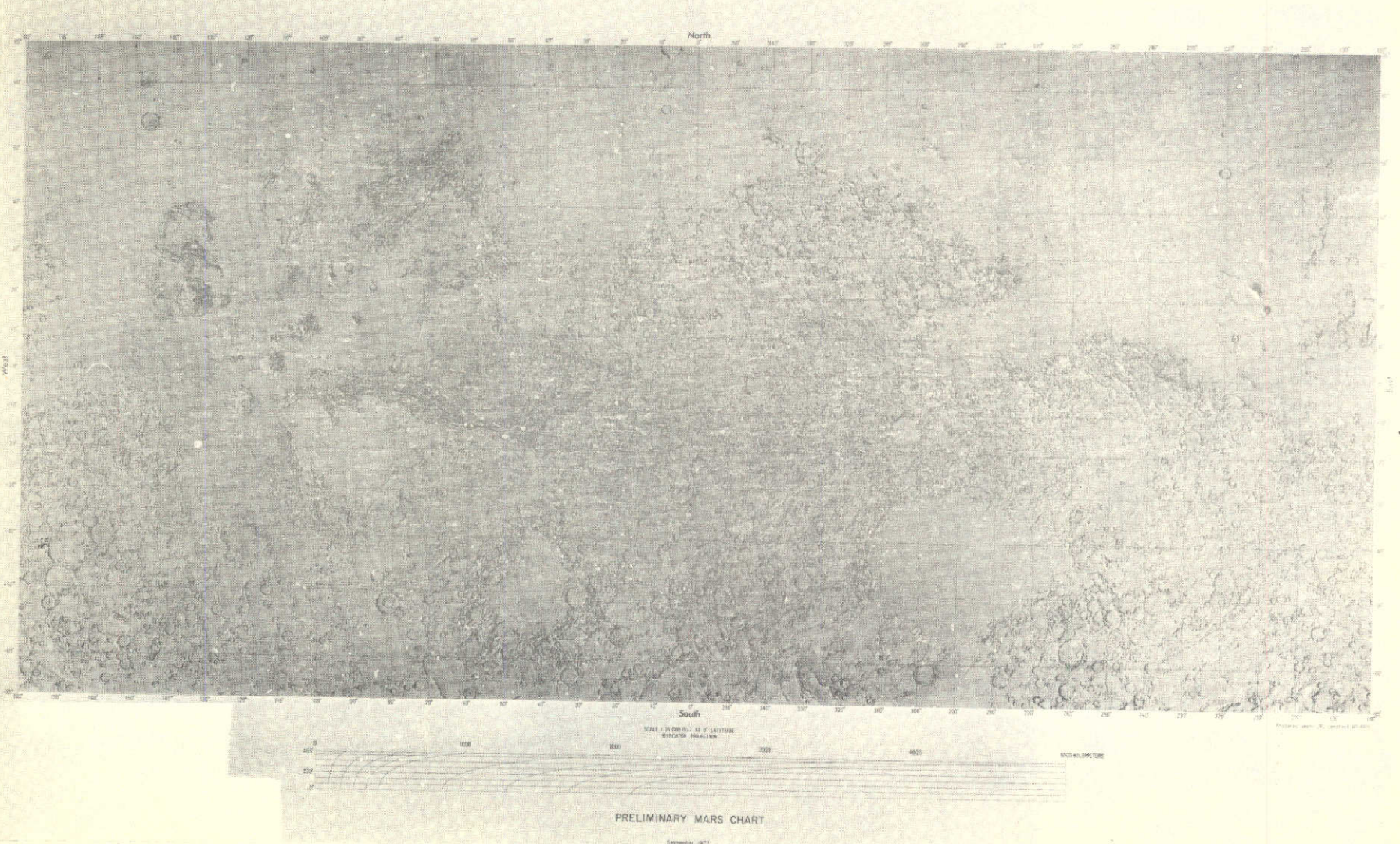


Figure 1. Shaded relief map based on Mariner 9 TV images (United States Geological Survey).

# MM '71 MARS PLANNING CHART

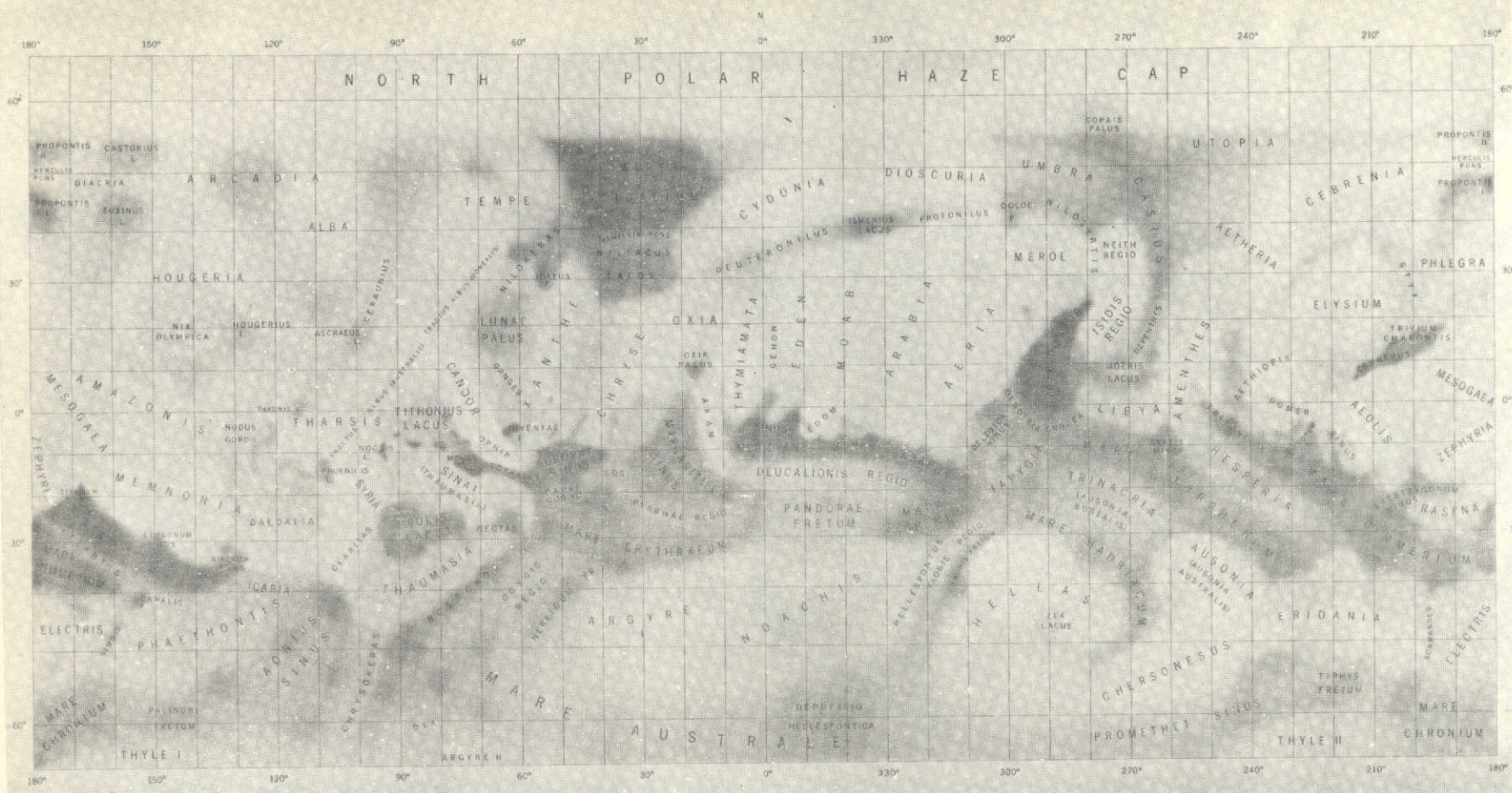


Figure 2. Earth-based albedo map of Mars (MM '71 Mars Planning Chart).

pattern: the multiringed basin (Wilhelms, 1973) has a rugged, dark mountainous rim surrounding a low, bright, nearly featureless plain. While this feature reproduces the terrestrial experience, it is nearly unique on Mars in the closeness of the correlation between topography and albedo, as shown below.

Mare Acidalium is a large, prominent dark region in the northern hemisphere in an area of smooth, mare-type plains. Sinus Meridiani, Sinus Sabaeus and Mare Serpentis are contiguous dark regions in heavily-cratered terrain. Much of very dark Syrtis Major lies in lightly-cratered smooth plains units. Dark Aurorae Sinus is located in canyonlands where few large craters survive.

Classical bright features corresponding to smooth, sparsely-cratered plains include Cebrenia, Elysium and Amazonis. Eden, Moab, Arabia and Aeria are adjacent bright regions lying in heavily-cratered terrain. Bright Tharsis not only includes the large constructional shield volcanoes, but also a complex region of intersecting faults, grabens and horsts. Elysium is a circular bright area of smooth plains in which a number of volcanic features are seen.

At this scale no simple relation is obvious. Therefore, a careful examination of some 100 classical albedo features was made using the two maps shown in Figures 1 and 2. For each area the kinds of terrain covered by the albedo feature were catalogued, and particular attention was paid to the contacts with other albedo features around the perimeter of the feature under examination. The study is essentially complete to the limit of the maps; i.e., between 50°N and 60°S for the (southern midsummer) season of the albedo map ( $L_s \approx 320^\circ$ ). All major features were examined,

including small regions like Juventae Fons and Noctis Lacus. The Mariner Mars '71 Planning Chart was chosen over other albedo maps (e.g., the Lowell Planetary Patrol Maps) for the sharpness of the boundaries between albedo features. Maps based principally on photography suffer from fuzziness of boundaries which becomes prohibitive in this kind of detailed study.

While it is beyond the scope of this paper to list the details of topography for all 100 features studied, the following statements can be made (with representative examples):

1. There is no simple relation between albedo and topography (terrain unit). Not all dark areas are cratered terrain; many bright areas are not smooth plains.
2. Several of the largest albedo features are dominated by a single kind of terrain. Hellas and Cebrenia are bright, smooth plains; Moab and Arabia are bright, heavily-cratered areas. Casius and Mare Acidalium lie on dark smooth plains; Sinus Meridiani and Sinus Sabaeus are dark, heavily-cratered regions.
3. Many classical albedo features consist of - or cross over - two or more geologic units. This occurs both in dark areas like Syrtis Major (smooth plains and cratered ridges) and Mare Erythraeum (heavily-cratered terrain to moderately-cratered plains) and in bright areas such as Amazonis (smooth terrain with emergent ridges and cratered terrain) and Amenthes (ridged cratered terrain and smooth, sparsely-cratered plains).
4. The boundaries between conspicuous albedo features often corresponds to a change in the surface topography. This may be a change in geologic unit or terrain type; e.g., from smooth plains to rugged mountains

(Moeris Lacus/Libya) or from troughed canyons to cratered plains (Aurorae Sinus/Eos). The change may also be more subtle, such as a series of aligned or contiguous ridges to mark the boundary (Daedalia/Claritas), or the rim of a very large crater (Sinus Sabaeus/Moab) or even a change in the density of moderately sized craters (Mare Cimmerium/Eridania). This boundary effect occurs in both hemispheres, but is more obvious in the southern, where the majority of dark region are found.

5. Some albedo boundaries occur where there is no discernable change in topography (at the scale of the maps) throughout the two features; examples include dark Utopia - bright Cebrenia which both lie on the same smooth plains unit, and the junctions of Moeris Lacus - Isidis Regio - Nepenthes which again all lie in the same smooth plains unit. Likewise, there is no change in the heavily-cratered terrain from the dark Mare Cimmerium into bright Electris.

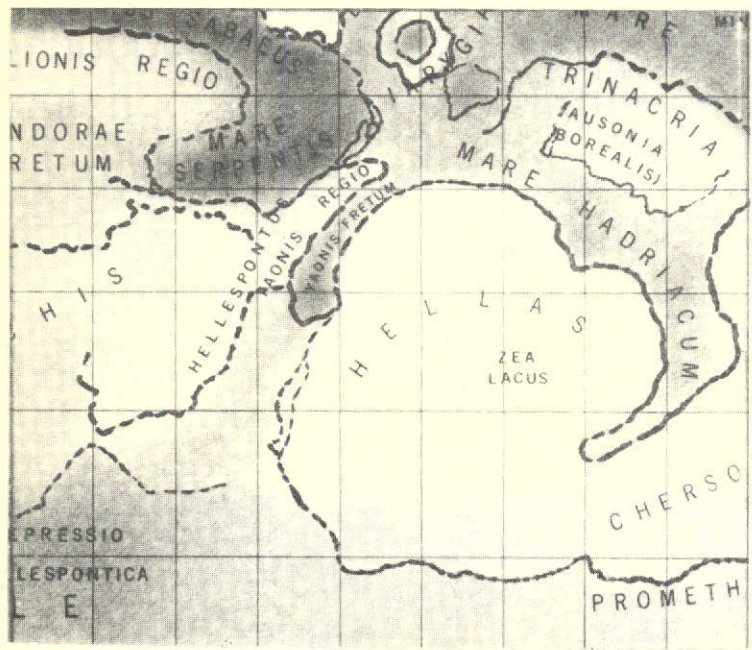
6. Several major albedo features are localized by structure; change in albedo corresponds to a distinct change in topography over most of the perimeter of the feature. Bright areas in this category include Hellas and Alba; dark areas are Lunae Palus and Aurorae Sinus. The first three of these are roughly circular in outline; the fourth lies in the complex canyonlands region.

7. Some albedo features would more exactly fit specific topographic features with a shift of less than  $2^\circ$  from their recorded positions on the Mars Planning Chart. For a region like Coprates, the required direction of shift of the albedo feature is north and east (this relocation would also align Phoenicis Lacus, Nodus Gordii and Pavonis Lacus with nearby structures). This observation, which applies mostly to small albedo features,

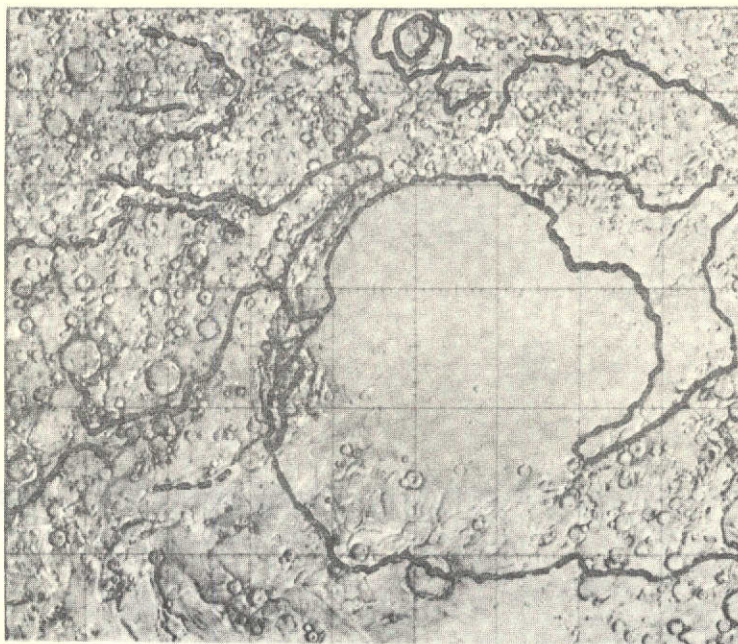
far from the central meridian, may reflect uncertainties in the coordinates of these regions. A change in the position of the polar axis and establishment of a uniform control net for Mars may reconcile this problem (see Davies and Arthur, 1973; de Vaucouleurs, et al., 1973). Recently published maps by Inge and Baum (1973) and de Vaucouleurs (1973) show the dark feature Coprates relocated within the canyon. The assumption of structural control implicit in these maps will require photometric reduction of the Mariner 9 imagery for confirmation.

Conclusions 1, 2, 3 and 5 are adequately demonstrated by comparison of Figure 1 with Figure 2. Figure 3 shows the Hellas region, from  $260^{\circ}$  to  $350^{\circ}$  W longitude and from  $-10^{\circ}$  to  $-65^{\circ}$  latitude. The excellent correspondence of albedo with topography is easily seen, especially along the north and western rim of the basin, in the region of dark Yaonis Fretum and western Mare Hadriacum. IRIS pressure maps (Conrath, et al., 1973; Hanel, et al., 1972) of this region show the bright desert portion Hellas to be a deep depression, while lower pressure contours follow the dark rim as well as does the topography. A three-way correlation exists here: smooth, sparsely-cratered plains are low and bright; rugged, cratered mountainous terrain is locally dark and relatively high. Topographic control of albedo is suggested (4, above).

The classical albedo features Syrtis Major, Meroe, Neith Regio, Isidis Regio, Nepenthes, Moeris Lacus and Libya are shown in Figure 4 ( $250^{\circ}$  W to  $300^{\circ}$  S,  $-10^{\circ}$  to  $+40^{\circ}$ ). The very dark feature Syrtis Major is observed to cross more than one terrain unit (3, above): the northern tip lies along ridges, the middle portion in relatively smooth plains. Topographic control (4, above) of the northern boundary is suggested; it

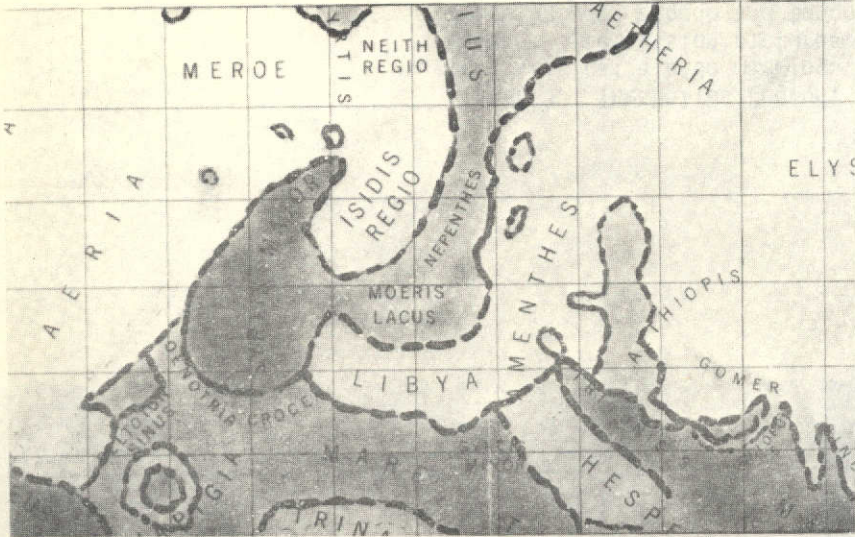


(a)

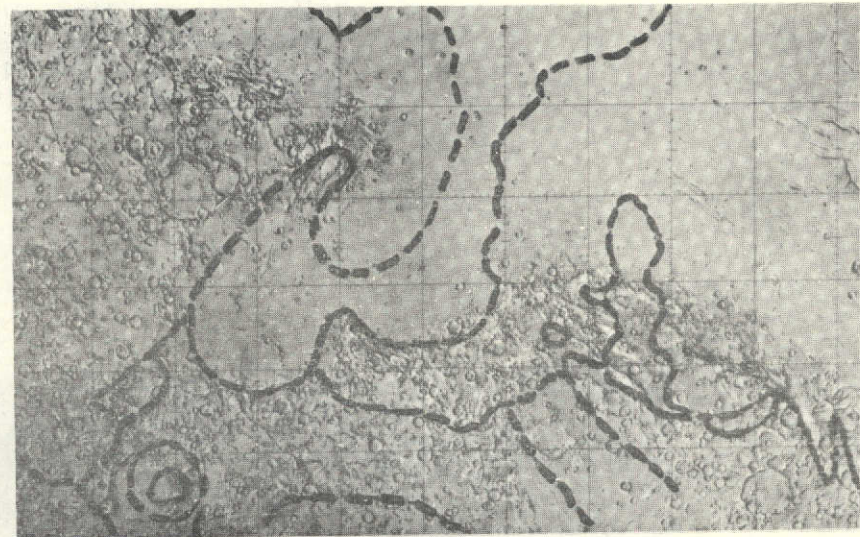


(b)

FIGURE 3. The Hellas Region. (a) Ground-based map showing the classical albedo markings. (b) Shaded relief map from Mariner 9 television pictures. Note the strong correspondence between albedo and topography along the west, northwest and northern run of the basin. This correlation (high, rugged, dark; low smooth, bright) does not hold for other albedo features shown in this figure.



(a)



(b)

FIGURE 4. Syrtis Major-Libya. (a) Ground-based albedo map. (b) Shaded relief map from Mariner 9 television pictures. Topographic control of the northern and southern boundaries of Syrtis Major is suggested. Albedo and topography correlate strongly at the Moeris Lacus-Libya boundary. This basin shows the inverse of the Hellas albedo-topography relation (see text). Note that both Amethes and Syrtis Major cross over major geologic units. There is little to suggest a topographic boundary along the Isidis Regio-Nepenthes albedo contact.

is obvious to the south where craters emerge from smooth plains at the border with brighter Oenotria Crocea.

There is also strong structural change corresponding to the albedo boundary between the dark smooth plains of Moeris Lacus and the brighter Libya region of rugged mountains. The multiringed basin Libya (Wilhelms, 1973) differs sharply from Hellas in that the mountainous rim is bright (it is dark in Hellas) while the central filled portion is dark (bright in Hellas).

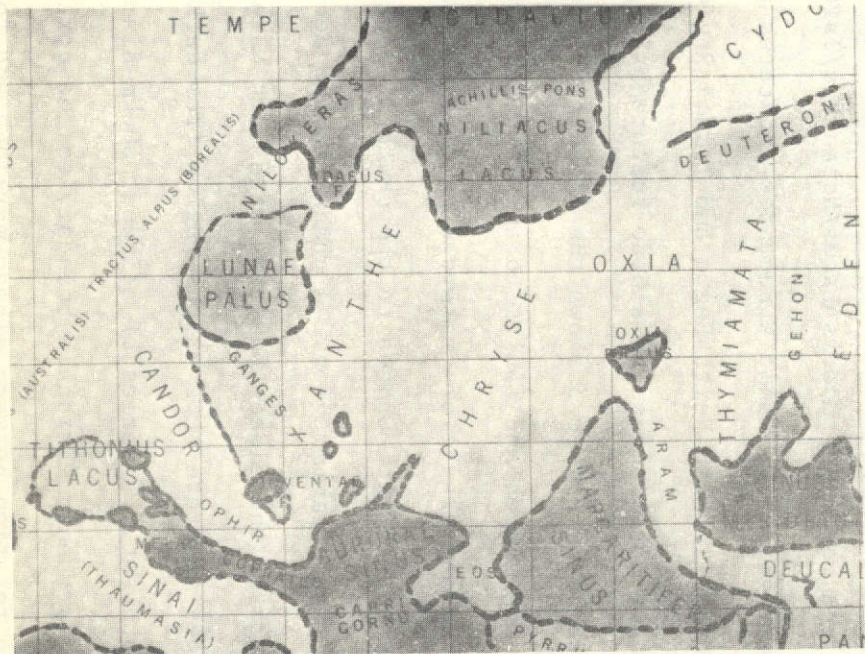
Amenthes is another example of an albedo feature that crosses geologic units (3, above). This bright area is rough, ridged terrain in the south, but becomes smooth plains to the north.

There is no topographic variation shown on the shaded relief map to mark the albedo change in the region of Moeris Lacus/Nepenthes/Isidis Regio (5, above). Only the appearance of volcanic structures indicates a change in the smooth plains in which lie both Neith Regio and Isidis Regio.

Lunae Palus is strongly localized as an albedo feature by topography around its perimeter (6, above). Figure 5 shows the close correspondence between albedo change and the ridges and faults to the west, northwest and far north. On the east, the appearance of craters signifies the boundary with brighter Xanthe. The border with Ganges to the south is indistinct.

Figure 6 represents the Eridania region. A change in the density of craters at about  $\sim 39^\circ$  indicates the albedo boundary with dark Mare Cimmerium (4, above). Parallel ridges separate this bright region from darker Promethei Sinus on the southwest. A series of aligned, 60 km-diameter craters suggests the Mare Tyrrhenium/Eridania boundary to the north.

It is clear that the relation between albedo markings and topography

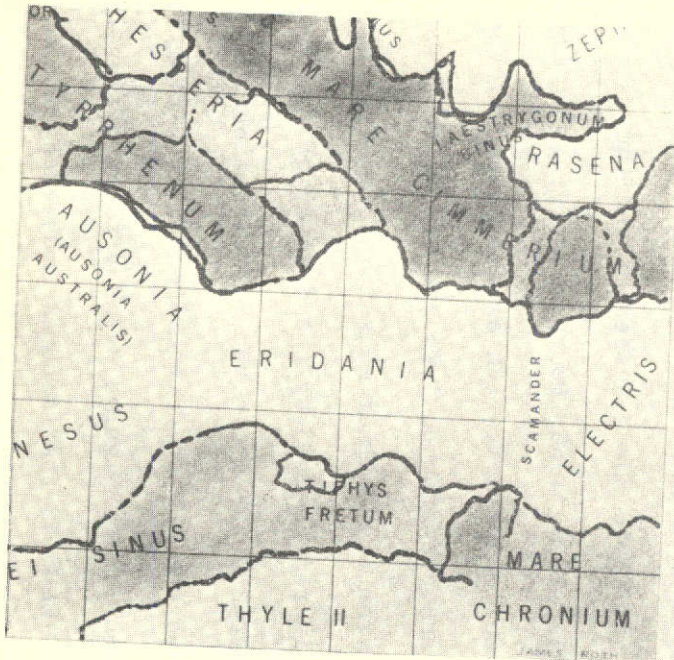


(a)

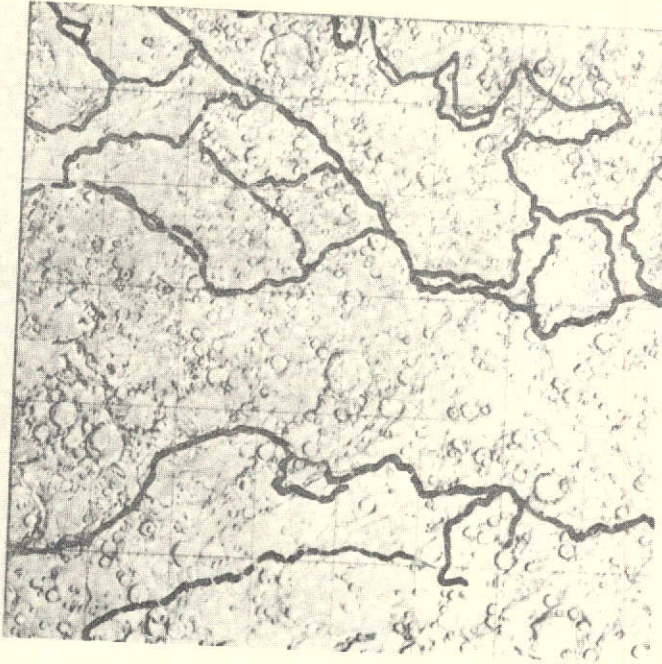


(b)

FIGURE 5. Lunae Palus. (a) Albedo map. (b) Mariner 9 shaded relief map. Note the localized nature of Lunae Palus. The albedo boundary corresponds to topographic features, especially along the western and northern borders. The classical canal Coprates, on the other hand, does not lie within the structural limits of the canyon (see text).



(a)



(b)

FIGURE 6. The Eridania region. (a) Classical albedo map. (b) Topographic features from Mariner 9 television. Crater density variations may correspond to the albedo contact between Eridania and Mare Cimmerium. The southern boundary with Promethei Sinus lies along a series of ridges.

is not a simple one. It is not possible to deduce the exact natures of the bright and dark regions from Mariner 9 television imagery alone. A similar conclusion was reached by Milmann (1973) in a more limited study.

ALBEDO AND REGIONAL ELEVATION.

Mariner 9 S-band occultation data (Kliore, et al., 1973; Kliore, et al., 1972) together with infrared (Conrath, et al., 1973; Hanel, et al., 1972) and ultraviolet (Hord, et al., 1972) pressure mapping have provided elevation information for much of Mars. The heavily-cratered southern portion of the planet in general lies some 3-4 kilometers higher than the smoother, northern plains. There are a few notable exceptions to this hemispherical generality: the very deep depression of the Hellas basin in the southern hemisphere and the uplifted volcanic complexes in Tharsis and Elysium in the northern hemisphere.

Radar profiles are now available for a number of latitude strips around Mars (Pettengill, et al., 1973, 1969; Downs, et al., 1973; Rogers, et al., 1970). To compare radar topography with albedo features, the classical bright and dark areas were grouped into one of six relative albedo categories determined from the Mariner Mars 1971 Planning Chart (Figure 2). Relative albedo is represented by the density of crosshatching: the greater the crosshatching the lower the relative albedo of the feature. Figure 7 displays the albedo categories and lists representative features for each category. In Figures 8 and 9 the radar profiles are overlain by the relative albedo of the features crossed by the radar beam. In all cases, the albedo strips were prepared first; radar points were added later to prevent biasing of the albedo boundaries.

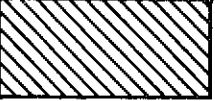
RELATIVE ALBEDO SCALE		REPRESENTATIVE AREAS
1		WHITE ELYSIUM, AMAZONIS, ZEPHYRIA
2		LIGHT GREY ARABIA, DAEDALIA, DEUCALIONIS REGIO
3		GREY EOS, GANGES, HESPERIA
4		DARK GREY LUNAE PALUS, MARGARITIFER SINUS
5		DARK AURORAE SINUS, TRIVIUM CHARONTIS
6		VERY DARK SYRTIS MAJOR, MERIDIANI SINUS

Figure 7. Relative albedo of classical martian albedo features. Based on the MM '71 Mars Planning Chart (de Vaucouleurs).

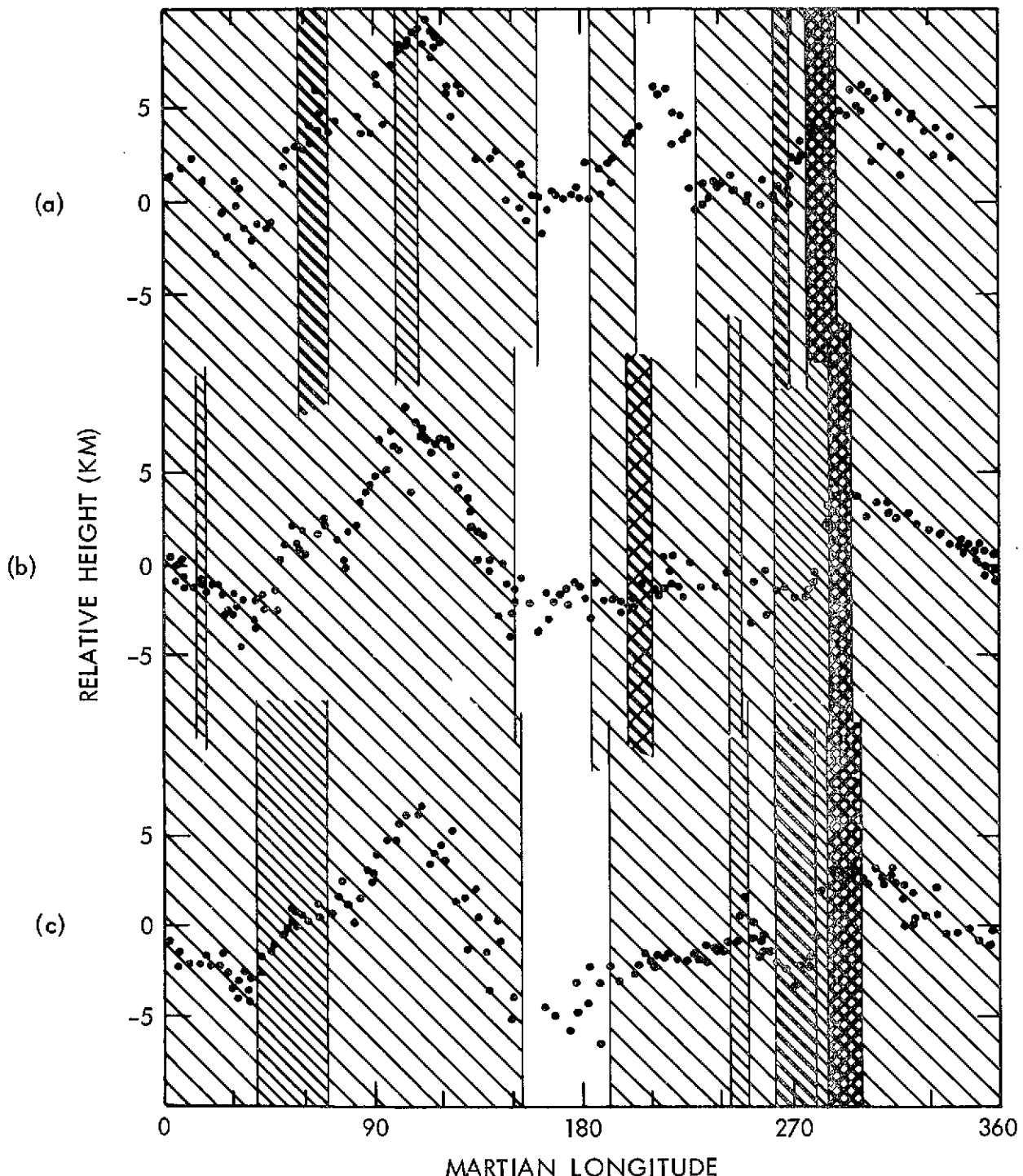


Figure 8. Radar profiles for three northern latitudes:

(a)  $22^\circ$  N; (b)  $11^\circ$  N; (c)  $6^\circ$  N. Cross-hatching indicates relative albedo (see text; also Figure 7). Radar data from Rogers, et al., 1970.

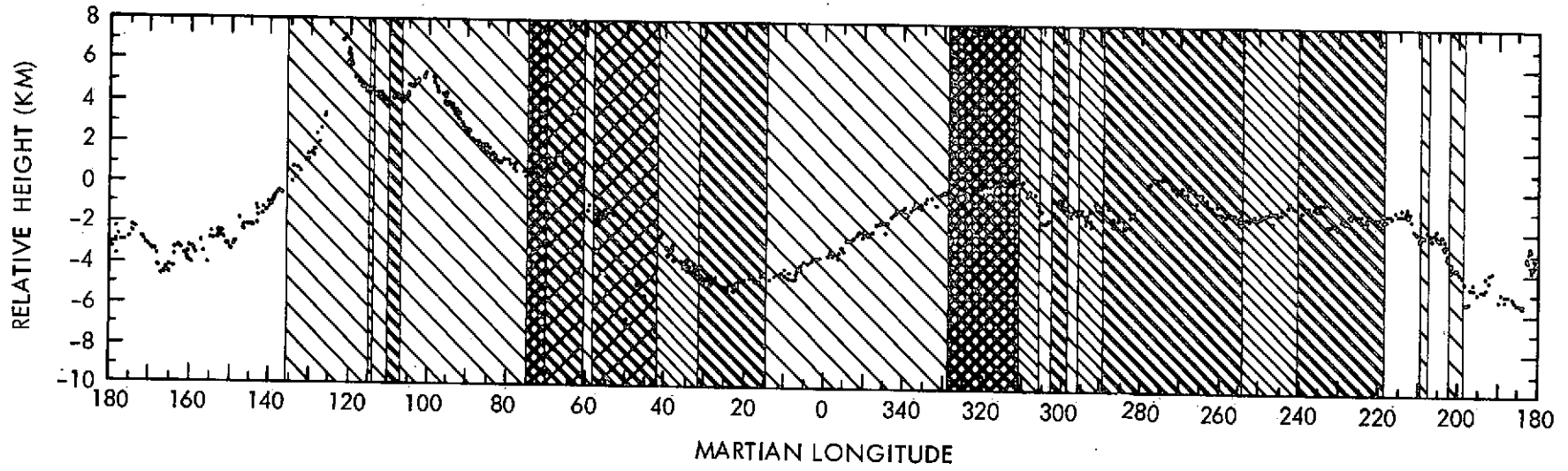


Figure 9. Southern hemisphere radar profile compared with relative albedo.  
Latitude approximately  $14^{\circ}$  S. From Pettingill, et al., 1973.

Figure 8 shows radar data for three latitude strips in the northern hemisphere of Mars (Rogers, *et al.*, 1970). Note that the longitude scale in this one figure runs left to right from  $0^\circ$  to  $360^\circ$ , contrary to the convention used in Figures 1, 2 and 9. The prominent high centered at  $110^\circ$  W is the Tharsis Ridge, on which lie the large Martian shield volcanoes. This area is bright, as is the secondary high at  $22^\circ$  N latitude corresponding to the Elysium volcanic complex ( $208^\circ$  to  $230^\circ$  W longitude). The bright low area between  $160^\circ$  and  $180^\circ$  W longitude is the Amazonis-Mesogaea region ( $6^\circ$  N), and the very dark uplifted region at  $285^\circ$  W is Syrtis Major.

Even at the low resolution of this data, the radar profile reflects the major topographic features of the shaded relief map (Figure 1). For example, the large shield volcano in Elysium is seen at longitude  $212^\circ$  W ( $22^\circ$  N latitude) as a peak in this uplifted region. Albedo features, on the other hand, show no correlation with elevation: there are both high and low bright regions, and dark areas also are both high and low. In some cases, however, a change in albedo does correspond to a distinct change in topography. The scarp eastward of  $285^\circ$  W longitude is reflected in a change in albedo (from very dark to dark grey in the relative scale used here) in the  $11^\circ$  latitude strip. The complex of ridges seen in Figure 1 at  $283^\circ$  W,  $+22^\circ$  is marked both in albedo and radar topography in Figure 8. The radar peak at  $6^\circ$  N,  $248^\circ$  W corresponds to a slight change in albedo, and is also seen in the shaded relief map of Figure 1. Considering the uncertainties in the positions of classical albedo features and the coarseness of the radar data, it is significant that topographic control of some albedo features is suggested.

A southern hemisphere radar trace at approximately  $14^\circ$  S latitude is shown in Figure 9. There is excellent agreement between radar features

and the structure shown in Figure 1. The southern extension of the Tharsis Ridge into Memnonia-Daedalia is obvious, as is the sharp relief of the canyonlands near 40° to 65° W. The large crater in Iapygia (304° W) is clear in the radar profile; other craters at 198° W, 230° W and 317° W are also clearly marked.

There are both low, bright regions (10° W, 160° W) and high, bright regions (100° W, 120° W). Dark areas are also both high (65° W, 275° W) and low (25° W, 42° W), though in general do not reach the extremes of elevation that bright features do. Hartman (1973a) has reached a similar conclusion. The dark spot Phoenicis Lacus occupies a low area (109° W) in a complex of ridges (see Figure 1) in a generally high and bright uplift of immense proportions (75° W to 135° W). The spot itself lies within the ridges seen in Figure 1; the bright material on either side is relatively smooth and sparsely-cratered. This is a strong case for topographic control of the albedo feature.

There are other examples of correspondance between topographic change and the border of albedo features in Figure 9. The steep scarp at 42° W lies along a distinct change in albedo (bright outside the canyon to dark within the depression). The relatively bright portion of Sinai (68° W) lying south of the canyon (Figure 1) shows a change in elevation in the radar data. The darker, central portion of Iapygia at 301° W corresponds to a slight peak while the adjacent bright areas (at 304° W and 295° W) are relatively low. The onset of a downhill slope westward of 319° W lies along the boundary between brighter Iapygia and darker Sinus Sabaeus. A steep upward rise to the west of 31° W occurs at the change from dark Margaritifer Sinus to brighter Eos.

It is beyond the scope of this paper to detail the albedo/topography boundary conditions for each classical albedo feature. Careful examination of such radar and other topographic data does yield the following conclusions:

1. There is no simple correspondance between albedo and regional elevation: dark and bright areas are both relatively high and low.
2. The very lowest and very highest regions on Mars are usually bright.
3. Boundaries between albedo features often correlate with topographic changes. These variations in elevation may be sudden (scarps, canyon walls) or gentle (change in slope or in direction of slope).

Hartmann (1973a) has also reached the first two conclusions in a very fine statistical analysis of the available topographic data.

Finally, it should be pointed out that an investigation of this nature requires careful examination of all the available data. It is possible, for example, to arrive at a totally erroneous apparent correlation between albedo and altitude by examining the single radar trace in Figure 8c. At this latitude, dark areas tend to be high; bright areas (except Tharsis) are generally lower. The Mariner 9 occultation and pressure-mapping data are useful in placing individual radar traces in global perspective. The conclusions of the section on "Albedo and Regional Structure" are supported by the available elevation data: the relation between albedo and topography is not a simple one.

DISCUSSION.

Sagan, et al. (1973, 1972), find that strong seasonal and secular albedo variations on Mars can be understood in terms of the production and destruction of crater wind tails. Bright streaks in the lee of craters probably result from the deposition of bright fines; dark tails may be the scouring of fines off darker subsurface material, or, in some cases, may be the deposition of dark material (Sagan, et al., 1972, Figure 27). Wind streaks are generally well correlated with dark albedo features (Sagan, et al., 1973, Figure 2). Secularly variable features lie mostly within smooth plains units, and the albedo variations are attributed to the variability of the (dark) streaks in these regions.

Several large, bright albedo features contain no streaks (bright or dark). From Figure 2 of Sagan, et al. (1973), the bright areas Amazonis-Mesogaea and Eden-Moab-Arabia-Aeria are noticeably absent of arrows; likewise Hellas, Argyre I and most of Elysium are without streaks. This cannot be an effect of topography only: Amazonis, Hellas and Elysium are primarily smooth plains units with Elysium relatively higher in elevation than Amazonis and Hellas. The Eden-Moab-Arabia-Aeria complex is a heavily-cratered region elevated to the height of Elysium. Elsewhere on the planet streaks are observed in all types of terrain, in bright areas and in dark areas, and at a variety of altitudes. It may be these streakless areas are well blanketed with fines, and there is no contrast between crater tails and the general material of the region. However, Soderblom, et al. (1973), find that, of these areas, only Argyre I, Hellas and the very northern part of Eden-Moab-Arabia-Aeria lie within the "mantled terrain" blanket; Amazonis, Mesogaea and Elysium, together with most of

Eden to Aeria, lie in unmantled terrain. Alternate explanations, such as the preferential scouring of fines from these bright features, must also be considered.

Scouring of bright fines to reveal darker subsurface material is observed in a variety of cases. The eastern boundary of Syrtis Major broadens seasonally, and downhill transport of fines in the prevailing wind direction is indicated (Sagan, et al., 1971). The regional dust storm observed in the Euxinus Lacus region by Leovy, et al. (1972) uncovered darker material in its wake. Some dark streaks, as well as some dark blotches, are most easily understood as dark deposits, but others seem to be the result of scouring of fines (Sagan, et al., 1972, Figure 27; Sagan, et al., 1973). Global dust storms indicate that planet-wide redistribution of bright material does occur. Despite this, the large dark albedo features of Mars have survived more or less unchanged during the 100 years of reliable earth-based observations, and perhaps longer.

It is possible that many, but not all, bright features on Mars are the result of accumulation of bright fines. The Hellas basin is a good candidate for such a feature. Indeed, part of the albedo difference between Hellas and Moeris Lacus (see second section, above) may result from the greater depth of the bright desert. Such an explanation becomes unlikely for sharply uplifted features, such as Elysium and Tharsus, both of which lie outside the "mantled terrain" mapped by Soderblom, et al. (1973). Indeed, to all appearances, the slopes of Nix Olympica and the other large volcanic features (both in Tharsis and Elysium) seem relatively fresh (Carr, 1973; Masursky, 1973).

It is unlikely that the classical dark areas of Mars are depositional features: the evidence for dark material transport suggest that it is far too limited to account for the extensive regions observed (Sagan, et al., 1973). Furthermore, the persistance of the dark areas throughout the observational history of Mars through numerous localized and global dust storms would require exceptional wind and settling conditions, for which there is no evidence. Dark areas are most likely exposed bedrock or material derived in situ from intrinsically dark crustal rock.

What is not clear is whether the bright material is the finely divided product of a darker parent material, or is derived from a rock type which is intrinsically bright. If all bright areas are accumulated fines, there exists the possibility that all the observed albedo features on Mars result from erosion and deposition of a single crustal unit. As shown before, it is not reasonable that all bright areas are dust traps, though some may be so. The alternative is to suggest two distinct types of crust, as mentioned by Masursky (1973). Bright albedo features contain both fine and coarse bright particles derived from intrinsically bright bedrock; the fines are mobile and can be transported onto (and off of) dark areas as described by Sagan and Pollack (1969).

The extensive northern plains units lack the large craters observed in the southern portions of Mars. Hartmann (1973b) suggests a factor of 10 difference in ages (crater retention ages) of the volcanic regions of Tharsis compared with the older, heavily-cratered uplands near the equator. Erosion rates estimated by Hartmann (1973b) suggest that the current erosion is much less than that which occurred before the Tharsis and Elysium areas were "resurfaced" (Hartman's term). The bright low-lands bear a strong morphological similarity to the lunar mare flows

(Carr, 1973). The evidence for a rock type distinct from that which floors dark cratered areas is compelling.

There is marginal spectral data suggesting compositional variations correlated with albedo. McCord and Westphal (1971) find a sequence of spectral reflectivity curves whose characteristics vary with decreasing albedo. Absorption bands near  $1.0\mu$  are deepest for the darkest areas observed, becoming weaker in the spectra of brighter areas. There is also the suggestion of a weak feature at  $0.85\mu$  in the spectra of some of the dark areas. Adams (1968) has attributed the  $1.0\mu$  feature to the  $\text{Fe}^{+2}$  ion in ferrosilicates, and suggests (Adams and McCord, 1969) a difference in the  $\text{Fe}^{+2}/\text{Fe}^{+3}$  ratio between dark Syrtis Major and bright Arabia. The total number of areas studied by these authors is too small to conclusively identify the compositional differences between bright and dark areas, but the spectral data is at least suggestive of distinct rock types.

In many of its physical characteristics, Mars lies intermediate between the now (essentially) inactive Moon and the ever-active Earth: size, mass, density, atmospheric structure, extent of volcanic and tectonic activity, and so on. The Earth and the Moon have both evolved two distinct types of crustal materials. The continental masses of the earth are granitic, while the ocean basins are floored by basalts. The highlands of the Moon are anorthositic gabbro; the mare regions are iron-rich basalts. Arguing by analogy is not always compelling, but there is strong evidence that such two-fold crustal formations are the normal occurrence for terrestrial planets (Lowman, 1973). Considering the marginal spectral data and the striking morphological evidence, it seems plausible that Mars has also generated two kinds of crustal materials.

The lack of geological correlation with albedo is still a puzzle: one might well expect all dark areas to be ancient, heavily-cratered uplands

or, as is the case of the moon, low, smooth mare-type plains. As shown in the second section, dark areas are both, and bright areas are also found on a variety of topographic units. The origin of the bright fines is still in question: finely-divided dark material is as plausible as finely-divided bright bedrock. Considering the extent of mixing that occurs on Mars, it is not surprising that the observed spectral differences between bright and dark areas are slight; more compositional data for a larger number of the classical features is required before a definitive answer to these problems is obtained.

#### CONCLUSIONS.

The available evidence indicates that there is no simple correlation between the classical markings of Mars and the topographic structure observed by Mariner 9. Albedo boundaries often do show correspondence with Topographic variations.

Marginal spectral data, crater retention ages, morphological comparisons and evolutionary theory suggest the Martian surface is made of two distinct kinds of crust, perhaps similar to the oceanic/continental crustal division of the earth. The origin of the bright, mobil fines is unclear, but the degree of mixing during global dust storms, the inferred extensive erosion of the past epoch, and the broad similarities of the spectral curves for some bright and dark areas may suggest that fines are derived from both kinds of albedo features.

The absence of wind streaks in some large, bright regions is puzzling. Nonetheless, there is much support for Wind-blown Dust models to explain seasonal and secular albedo variations.

Further work is needed in several areas:

1. More spectral data from a variety of terrain units of different albedos is required to investigate the compositional natures of the classical features.
2. Higher resolution topographic data, and good altimetry or orbital radar mapping of large areas of Mars is desirable.
3. Detailed study of the available high resolution imagery of the bright/dark region boundaries will help resolve the importance of deposition and erosion in controlling the extent of classical features.
4. Finally, continued monitoring of the classical features and the martian surface from the Earth and from martian orbit is necessary to fully appreciate the complex nature of this active and exciting planet.

ACKNOWLEDGEMENTS.

Special thanks go to P.D. Lowman for suggesting this project, for a critical review of the manuscript, and for continued interest and encouragement throughout the study. M.F. A'Hearn also contributed several useful suggestions. This work was supported by NSF Grant NGL-21-002-033.

## REFERENCES

- Adams, J.B., 1968, Lunar and Martian Surfaces: Petrologic Significance of Absorption Bands in the Near Infrared, *Science* 159, 1453.
- Adams, J.B. and McCord, T.B., 1969, Mars: Interpretation of Spectral Reflectivity of Light and Dark Regions, *J. Geophys. Res.* 74, 4857.
- Adler, I., Trombka, J.I., Lowman, P., Schmadebeck, R., Blodget, H., Eller, E., Yin, L., Lamothe, R., Osswald, G., Gerard, J., Gorenstein, P., Bjorkholm, P., Gursky, H., Harris, B., Arnold, J., Metzger, A., and Reedy, R., 1973, Appolo 15 and 16 Results of the Integrated Geochemical Experiment, *The Moon* 7, 487.
- Binder, A.B., and Cruikshank, D.P., 1966, The Composition of the Surface Layer of Mars, *Commiss. Lunar Planet. Lab.* 4, 111.
- Binder, A.B. and Jones, J.C., 1972, Spectrophotometric Studies of the Photometric Function, Composition and Distribution of Surface Materials of Mars, *J. Geophys. Res.* 77, 3005.
- Carr, M.H., 1973, Volcanism on Mars, *J. Geophys. Res.* 78, 4049.
- Carr, M.H., Masursky, H. and Saunders, R.H., 1973, A Generalized Geologic Map of Mars, *J. Geophys. Res.* 78, 4031.
- Conrath, B., Curran, R., Hanel, R., Kunde, V., Maguire, W., Pearl, J., Pirraglia, J., Welker, J. and Burke, T., 1973, Atmospheric and Surface Properties of Mars obtained by Infrared Spectroscopy on Mariner 9, *J. Geophys. Res.* 78, 4267.
- Davies, M.E. and Arthur, W.G., 1973, Martian Surface Coordinates, *J. Geophys. Res.* 78, 4355.
- de Vaucouleurs, G., 1973, High Resolution Mars Albedo Maps, *Sky and Telescope* 46, 141.
- de Vaucouleurs, G., Davies, M.E. and Sturms, F.M., Jr., 1973, Mariner 9 Areographic Coordinate System, *J. Geophys. Res.* 78, 4395.
- Dollfus, A., 1961, Polarization Studies of the Planets, in The Solar System, Vol. 3, ed. G.P. Kuiper and B.M. Middlehurst, p. 343.
- Downs, G.S., Goldstein, R.M., Green, R.R., Morris, G.A. and Reichley, P. E., 1973, Martian Topography and Surface Properties as Seen by Radar: The 1971 Opposition, *Icarus* 18, 8.
- Hanel, R., Conrath, B., Hovis, W., Kunde, V., Lowman, P., Maguire, W., Pearl, J., Pirraglia, J., Prabhakara, C., Schlachman, B., Levin, G., Straat, P. and Burke, T., 1972, Investigation of the Martian Environment by Infrared Spectroscopy on Mariner 9, *Icarus* 17, 423.

Hartmann, W.K., 1973a, Martian Surface and Crust: Review and Synthesis, *Icarus* 19, 550.

Hartmann, W.K., 1973b, Martian Cratering 4, Mariner 9 Initial Analysis of Cratering Chronology, *J. Geophys. Res.* 78, 4096.

Hord, C.W., Barth, C.A., Stewart, A.J. and Lane, A.L., 1972, Mariner 9 Ultraviolet Spectrometer Experiment: Photometry and Topography of Mars, *Icarus* 17, 443.

Inge, J.L. and Baum, W.A., 1973, A Comparison of Martial Albedo Features with Topography, *Icarus* 19, 323.

Kliore, A.J., Cain, D.L., Fjeldbo, G., Seidel, B.L., Sykes, H.J. and Rasool, S.I., 1972, The Atmosphere of Mars from Mariner 9 Radio Occultation Measurements, *Icarus* 17, 484.

Kliore, A.J., Fjeldbo, G., Seidel, B.L., Sykes, H.J., and Woiceshyn, P.M., 1973, S Band Radio Occultation Measurements of the Atmosphere and Topography of Mars with Mariner 9: Extended Mission Coverage of Polar and Intermediate Latitudes, *J. Geophys. Res.*, 78, 4331.

Leovy, C., Briggs, G., Yang, A.T., Smith, B.A., Pollack, J., Shipley, E. and Wildey, R., 1972, Mariner 9 Television Experiment: Progress Report on Studies of the Mars Atmosphere, *Icarus* 17, 373.

Lowman, P.D., 1973, manuscript submitted to Journal of Geology.

Lowman, P.D. and Tiedemann, H.A., 1971, Terrain Photography from Gemini Spacecraft: Final Geologic Report, NASA X-Document 644-71-15.

Masursky, H., 1973, An Overview of the Geologic Results from Mariner 9, *J. Geophys. Res.* 78, 400.

McCauley, J.F., Carr, M.H., Cutts, J.A., Hartmann, W.K., Masursky, H., Milton, D.J., Sharp, R.P. and Wilhelms, D.E., 1972, Preliminary Mariner 9 Report on the Geology of Mars, *Icarus* 17, 289.

McCord, T.B. and Westphal, J.A., 1971, Mars: Narrow Band Photometry, from 0.3 to 2.5 Microns, of Surface Regions During the 1969 Apparition, *Astrophys. J.*, 168, 141.

Milman, P.M., 1973, The Traditional Features of Mars Compared with the Geologic Map of the Planet, *R.A.S.C. Jour.* 67, 115.

Neugegauer, G., Münch, G., Kieffer, H.H., Chase, S.C. and Miner, E., 1971, Mariner 1969 Infrared Radiometer Results: Temperatures and Thermal Properties of the Martial Surface, *Astron. J.* 76, 719.

Öpik, E.J., 1966, The Martian Surface, *Science* 153, 255.

- Pettengill, G.H., Shapiro, I.I. and Rogers, A.E.E., 1973, Topography and Radar Scattering Properties of Mars, *Icarus* 18, 22.
- Pettengill, G.H., Counselman, C.C., Rainville, L.P. and Shapiro, I.I., 1969, Radar Measurements of Martian Topography, *Astron. J.* 74, 461.
- Pollack, J.B. and Sagan, C., 1967, Secular Changes and Dark Area Regeneration on Mars, *Icarus* 6, 434.
- Rea, D.G. and O'Leary, B.T., 1965, Visible Polarization Data of Mars, *Nature* 206, 1138.
- Rogers, A.E.E., Ash, M.E., Counselman, C.C., Shapiro, I.I. and Pettengill, G.H., 1970, Radar Measurements of the Surface Topography and Roughness of Mars, *Radio Sci.* 5, 465.
- Sagan, C., Phaneuf, J.P. and Ihnat, M., 1965, Total Reflection Spectrophotometry and Thermogravimetric Analysis of Simulated Martian Surface Materials, *Icarus* 4, 43.
- Sagan, C. and Pollack, J.B., 1969, Windblown Dust on Mars, *Nature* 223, 791.
- Sagan, C., Veverka, J. and Grerasch, P., 1971, Observational Consequences of Martian Wind Regimes, *Icarus* 15, 253.
- Sagan, C., Veverka, J., Fox, P., Dubisch, R., Lederberg, J., Levinthal, E., Quain, L., Tucker, R., Pollack, J.B. and Smith, E.A., 1972, Variable Features on Mars: Preliminary Mariner 9 Results, *Icarus* 17, 346.
- Sagan, C., Veverka, J., Fox, P., Dubisch, R., French, R., Gierasch, P., Quann, L., Lederberg, J., Levinthal, E., Tucker, R., Eross, B. and Pollack, J.B., 1973, Variable Features on Mars 2, Mariner 9 Global Results, *J. Geophys. Res.* 78, 4163.
- Salisbury, J.W., 1966, The Light and Dark Areas of Mars, *Icarus* 5, 291.
- Sinton, W.M., 1967, On the Composition of Martian Surface Materials, *Icarus* 6, 222.
- Soderblom, L.A., Kriedler, T.J. and Masursky, H., 1973, Latitudinal Distribution of a Debris Mantle on the Martian Surface, *J. Geophys. Res.* 78, 4117.
- Van Tassel, R.A. and Salisbury, J.W., 1964, The Composition of the Martian Surface, *Icarus* 3, 264.
- Wilhelms, D.E., 1973, Comparison of Martian and Lunar Multiringed Basins, *J. Geophys. Res.* 78, 4084.
- Younkin, R.L., 1966, A Search for Limonite Near Infrared Spectral Features on Mars, *Astrophys. J.* 144, 809.